Colossal Magnetodielectric Effects in $DyMn_2O_5$

N. Hur, S. Park, P. A. Sharma, S. Guha, and S-W. Cheong
Department of Physics & Astronomy, Rutgers University, Piscataway, New Jersey 08854, USA
(Received 19 January 2004; published 3 September 2004)

We have investigated the detailed magnetic field dependence of the electric polarization and dielectric constant in (Tb, Dy, Ho)Mn_2O_5 where magnetic and ferroelectric transitions are intimately coupled. Our fundamental discovery is the unprecedented large change of the dielectric constant with magnetic field, particularly in $DyMn_2O_5$, associated with an unusual commensurate-incommensurate magnetic transition. This extraordinary effect appears to originate from the high sensitivity of the incommensurate state to external perturbation.

DOI: 10.1103/PhysRevLett.93.107207 PACS numbers: 75.80.+q, 75.47.Lx, 77.80.–e

Tuning the dielectric properties of materials with a magnetic field (H), electric voltage, or preparation conditions has been both scientifically important and technologically demanding [1–3]. For example, the novelty is evident if one can readily adjust the resonant frequency of a capacitive resonator with field-tunable dielectrics.

In order to magnetically control the dielectric or capacitance properties [4–6], two main strategies have been employed: controlling the interface physics in multilayer systems and amplifying the magnetodielectric (MD) effect near (ferro)magnetic transitions in (ferro)magnetic dielectrics. (In fact, the development of devices based on *magnetoresistance* effects follows very similar ideas: compare these dielectric strategies with the discoveries of giant magnetoresistance which is achieved by modifying the interfacial spin scattering in H and colossal magnetoresistance, which originates from a strong coupling between electronic transport properties and ferromagnetic (FM) order [7–9].) For example, the capacitance of a $Pd/AlO_x/Al$ film structure varies with H due to a spin-dependent electrochemical potential at the Pd surface [10]. MD effects in $BiMnO_3$ and $SeCuO_3$ represent the second strategy well. $BiMnO_3$ is ferroelectric (FE) below ~800 K and becomes FM at 105 K [11]. In the case of insulating, but non-FE $SeCuO_3$, a FM transition occurs near 25 K [12]. In both systems, there are weak but well-defined anomalies in the dielectric constant near the FM transition T. Unfortunately, the MD effect in all these systems turns out to be minute: the dielectric constant changes by less than 1% for H of several tesla. However, a new class of multiferroic material, $TbMnO_3$, has recently been found to produce a large MD effect of ~10%, associated with a 90° rotation of P by application of H [13].

Herein, we report significant MD effects near a unique commensurate-incommensurate magnetic transition in orthorhombic (Tb, Dy, Ho)Mn_2O_5 where magnetic transitions are intricately coupled with dielectric transitions. In particular, we discovered that the MD effect for $DyMn_2O_5$ is more than 100% in a broad T range below 20 K. This "colossal magnetodielectric" (CMD) effect clearly demonstrates an intriguing interplay between spin and lattice degrees of freedom as well as the extraordinary nature of a unique commensurate-incommensurate magnetic transition in RMn_2O_5 [14].

Single crystals of RMn_2O_5 (R = Tb, Dy, and Ho) were grown using B_2O_3-PbO-PbF_2 flux in a Pt crucible. The mixture was held at 1280 °C for 15 h and then slowly cooled down to 950 °C at a rate of 1 °C per hour [15]. For the dielectric constant and polarization measurement, we used thin rectangular specimens of single domain crystals (a cross sectional area of 1–2 mm^2 and a thickness of 0.15–0.2 mm), carefully chosen by utilizing a polarized optical microscope. Dielectric constants were measured by an LCR meter at various frequencies of 1–100 kHz with an excitation of 1 V. The dielectric loss (of the order of 10^{-3}) and frequency dependence of the dielectric constant were negligible in the above frequency range below 60 K. Specific heat (C_p) was measured using the standard relaxation method with a Quantum Design Physical Property Measurement System. Magnetization (M) was measured using a SQUID magnetometer.

The specific heat data in Fig. 1(a) show a number of successive phase transitions in RMn_2O_5. The phase transitions indicated by arrows have been identified from our experimental data of C_p, M, and dielectric properties as well as from the previously published results [14,16]. All three systems undergo a similar set of consecutive phase transitions with slightly different transition T. Long-range antiferromagnetic (AFM) order of the Mn^{3+}/Mn^{4+} spins is known to occur at T_N, and subsequently the FE transition happens at a T_C slightly below T_N. It has been proposed that the long-range magnetic ordering of Mn^{3+}/Mn^{4+} induces the FE transition via an additional Jahn-Teller distortion of Mn^{3+} ions [16]. RMn_2O_5 is characterized by the existence of another magnetic transition at T_N' around 19–27 K, at which commensurate AFM ordering becomes "incommensurate" [14]. It is also known that the AFM-type ordering of the rare earth ions occurs at $T_N(R)$ below ~10 K.

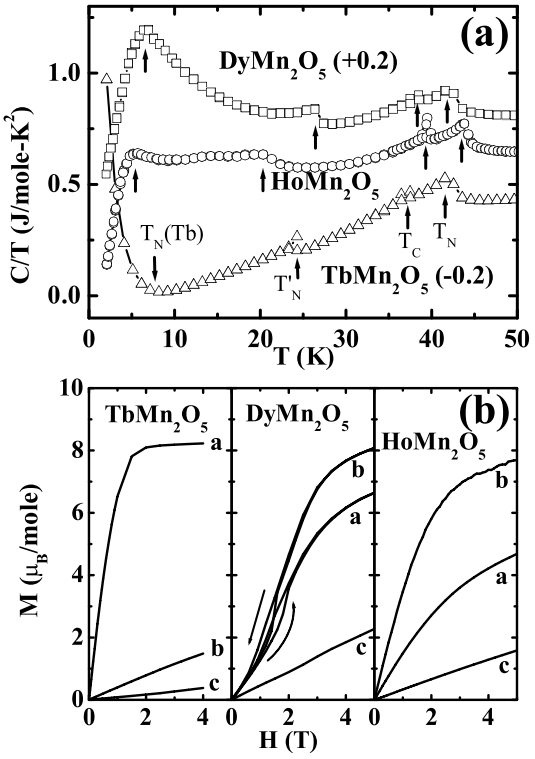

FIG. 1. (a) Specific heat, $C_p(T)$, of $TbMn_2O_5$, $DyMn_2O_5$, and $HoMn_2O_5$. Arrows indicate a number of low T phase transitions. $DyMn_2O_5$ ($TbMn_2O_5$) data were shifted by $+0.2$ (-0.2) J/mol K^2 for clarity. (b) Magnetization versus magnetic field at 3 K along the three principal crystallographic directions for $TbMn_2O_5$, $DyMn_2O_5$, and $HoMn_2O_5$.

$M(H)$ curves at 3 K for (Tb, Dy, Ho)Mn_2O_5 in Fig. 1(b) demonstrate the presence of significant magnetic anisotropy [17–19]. The data in this figure, combined with the results in the literature, indicate that the magnetic easy direction systematically varies with the size of the rare earth ion in RMn_2O_5. The magnetic easy direction of $TbMn_2O_5$ is along the a axis, that of (Dy, Ho)Mn_2O_5 is along the b axis, and that of Er(Tm)Mn_2O_5 is along the c axis [20]. Note that because of this general trend the Dy system is most magnetically isotropic in the a-b plane and that M of $DyMn_2O_5$ linearly increases in low fields, shows a kink at 1.5–2 T, and then slowly saturates for the a or the b direction for H above 3 T, indicating the presence of an H-induced phase transition at 1.5–2 T.

An extraordinary change in the dielectric constant, ε, with H of $DyMn_2O_5$ is displayed in Figs. 2(a) and 2(b). The zero-H ε exhibits features that closely match those found in C_p/T vs T in Fig. 1(b); i.e., it starts to increase at $T_N \approx 43$ K, exhibits a sharp peak at $T_C \approx 39$ K, and shows steplike anomalies at $T_N' \approx 27$ K and at $T_N(\mathrm{Dy}) \approx 8$ K. These clear dielectric anomalies, occurring at each magnetic transition, undoubtedly indicate a significant spin/lattice coupling, compared to the much more subtle dielectric anomaly at the FM transition temperature in

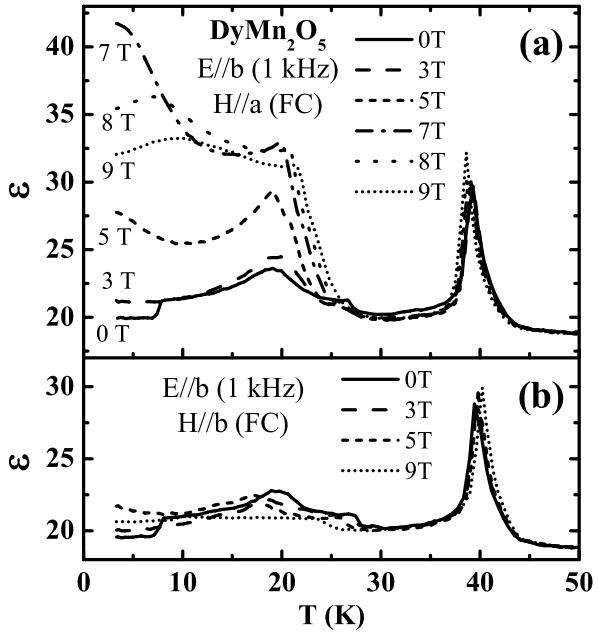

FIG. 2. (a) T dependence of the dielectric constant at 1 kHz along the b axis in various magnetic fields applied along the a axis, measured after cooling the sample in the presence of the same H [field cooling (FC)]. (b) Dielectric constant along the b axis in H applied along the b axis.

$BiMnO_3$, a prototypical ferroelectric and ferromagnetic system [11]. In addition, there exists another broad bump in ε at $\sim$19 K. The most striking feature is the large H dependence of ε below T_N' when H is applied along the a axis. The steplike anomaly at $T_N(\mathrm{Dy}) \approx 8$ K is smeared out with increasing H. On the other hand, the broad bump at $\sim$19 K becomes sharper and moves to higher T while the magnitude of ε drastically increases below T_N' with increasing H. The dielectric constant exhibits a maximum change of $\sim$109% at 3 K by the application of 7 T. To our knowledge, this is a record-high change of ε with H [13,21]. When H was applied along the b axis, as shown in Fig. 2(b), the effect of H on ε is significant, but not as large as that for the a axis even though the magnetic easy direction is along the b axis. Note that H along the b axis suppresses the anomaly at T near $\sim$27 K and also smears out the anomalies at $\sim$19 and $\sim$8 K.

As depicted in Figs. 3(a)–3(c), $\varepsilon(T)$ of all three (Tb, Dy, Ho)Mn_2O_5 systems in $H = 0$ exhibits both a sharp peak at around 40 K (the onset of ferroelectricity) and a steplike anomaly at T_N'. The H dependence $\varepsilon(T)$ of all three crystals also shows several common features: (i) FE T_C shifts to slightly lower T with increasing H, (ii) the steplike anomaly T at 19–27 K considerably increases with increasing H, and (iii) a large MD effect is observed near or below T_N'. However, the magnitude and the sign of the MD effect near or below T_N' depend on the system as well as T. The largest change in ε with H is 22(40)% near T_N' for Tb(Ho)Mn_2O_5 in 9 T and 109% at

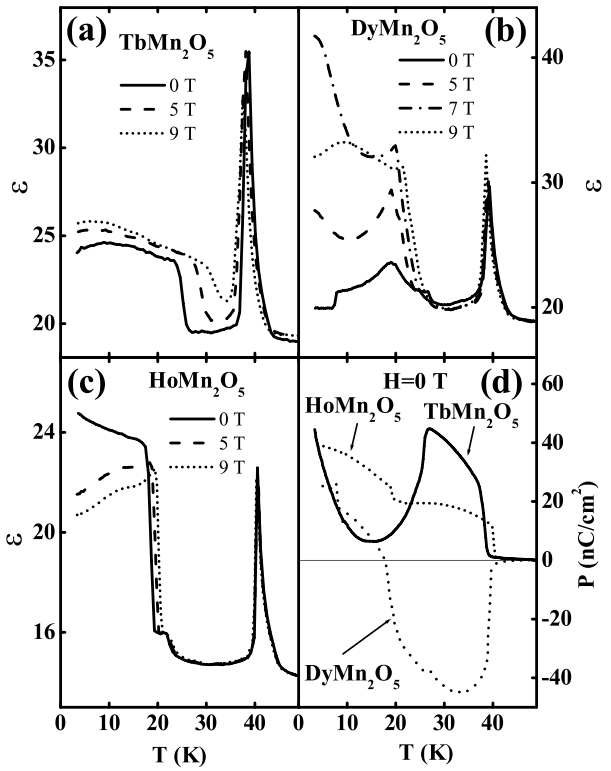

FIG. 3. T dependence of the dielectric constant of (a) $TbMn_2O_5$, (b) $DyMn_2O_5$, and (c) $HoMn_2O_5$ in various H. The dielectric constant was measured along the b axis and H was applied along the a axis for all three crystals. (d) Spontaneous polarizations of three crystals measured along the b axis in zero H.

3 K for $DyMn_2O_5$ in 7 T. It should be noted that the measured MD effects on these crystals were highly reproducible and also consistent with those on stoichiometric polycrystalline samples if one takes into account the angular averaging in polycrystalline specimens.

The spontaneous polarization (P) of all three crystals in zero H, displayed in Fig. 3(d), starts to increase at T_C and shows a peculiar anomaly near T_N'. The absolute value of P suddenly increases for $HoMn_2O_5$ or decreases for (Tb, Dy)Mn_2O_5 below T_N'. This complicated $P(T)$ behavior can be understood using the concept of ferrielectricity, in which the net P is composed of more than one component [22–24]. Ferrielectricity, which has occasionally appeared in systems with inherent structural complexity allowing crystallographically inequivalent sublattices, can also be indicated by the low measured value of P in comparison to conventional ferroelectrics and the sign change of P with varying T in $DyMn_2O_5$ due to the different temperature dependence of each polarization component [23,24]. We propose that the net P for these systems is composed of primarily two components: one component appearing below T_C and another component below T_N'. These components coexist below T_N', and they are collinear since no P component along the a and c axes was detected. Judging from the differences in the shape of $P(T)$, we also propose that these two components are parallel to each other for $HoMn_2O_5$ but antiparallel for Tb(Dy)Mn_2O_5. This model is consistent with the postulated presence of a two-well potential corresponding to two lattice-distortion configurations with almost equal energies in $EuMn_2O_5$ [16].

The change in ε, $\Delta\varepsilon/\varepsilon_0$, as a function of applied H of $DyMn_2O_5$ at 3 and 20 K is displayed in Fig. 4(a). As described previously, the maximum change of $\varepsilon(T)$ in fixed fields reaches 109% at 3 K for magnetic FC and the isothermal effect for zero-magnetic field cooling (ZFC) is slightly less, but still quite large at ~90%. The maximum of $\Delta\varepsilon/\varepsilon_0$ is reduced to ~40% at 20 K.

Figure 4(b) displays the change of the electric P by applied H at 3 K. The electric P shows an abrupt change at ~1.8 T and a hysteresis, closely related to the H dependence of $M(H)$ and $\Delta\varepsilon/\varepsilon_0$ at 3 K shown in Figs. 1(b) and 4(a), respectively.

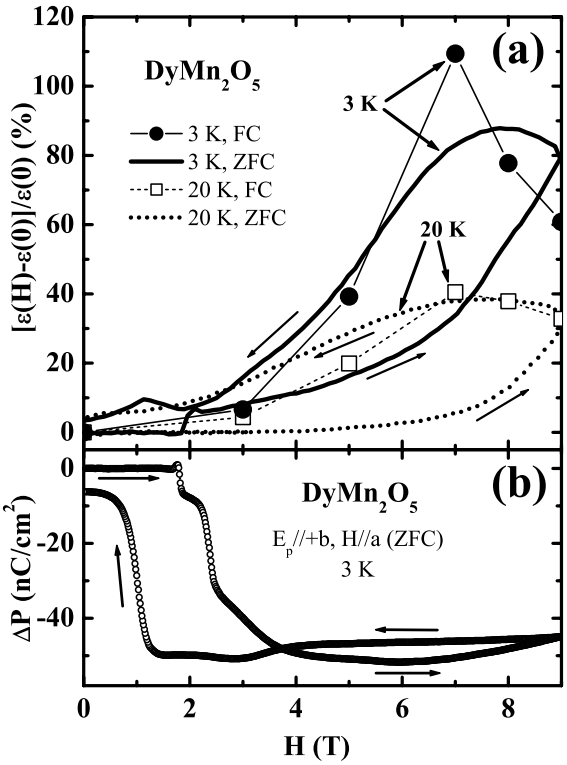

FIG. 4. (a) Change of dielectric constant vs applied H of $DyMn_2O_5$ crystal at 3 and 20 K. The solid and dashed lines indicate $\Delta\varepsilon/\varepsilon_0$ at 3 and 20 K, respectively, in increasing and decreasing H after ZFC, and the solid and open symbols indicate the FC data taken from $\varepsilon(T)$ in Fig. 2(a). (b) Change of the electric polarization by applied H at 3 K. Before the polarization measurement, the sample was cooled from 120 to 3 K in a static electric field, $E_p = 5$ kV/cm, and the magnetoelectric current was measured while increasing the magnetic field at a rate of 100 Oe/sec.

Several systematic trends in the physical properties appear to underlie the origin of the CMD effect in $R\mathrm{Mn_2O_5}$. The steplike increase of ε, the anomalous T dependence of P, and the large H effect on ε as well as P all appear below T_N', rather than T_N. Two P components also develop below T_N' in our ferrielectric model. T_N' turns out to be associated with a commensurate-incommensurate transition. The commensurate AFM transition [modulation wave vector of $(1/2, 0, 1/4)$] occurs at FE $T_C \approx 40$ K but becomes incommensurate with a modulation wave vector of $(1/2 - \delta, 0, 1/4 + \gamma)$ ($\delta \approx 0.02$ and $\gamma \approx 0.04$ in $\mathrm{YMn_2O_5}$) for T below 19–27 K at which another dielectric anomaly is present [14,25]. This is very surprising in that the typical incommensurate-commensurate transition results in the commensurate state being the low-T ground state. This is a consequence of the "locking in" of magnetic and lattice modulations that is energetically favored at low T [26,27]. Thus, the unusual incommensurate magnetic phase coincides with the appearance of multiple P components, large lattice polarizability, and an enormously large MD effect.

It is noteworthy that a significant magnetoelectric (ME) effect in the "commensurate" phase of $\mathrm{TbMnO_3}$ occurs above 5 T when P rotation occurs [13]. On the other hand, the ME effect in much lower fields (1–2 T) in the incommensurate phase for $\mathrm{DyMn_2O_5}$ certainly suggests the importance of incommensurability. Evidently, the presence of magnetic ions on the R site of $R\mathrm{Mn_2O_5}$ is also essential for the occurrence of large ME effects in low H if we compare our results to the observed ME effect in much higher fields (above 10 T) in $\mathrm{EuMn_2O_5}$ [28].

The enhanced MD effect in $\mathrm{DyMn_2O_5}$ relative to the Tb and Ho systems is consistent with these observations. First, $\mathrm{DyMn_2O_5}$ exhibits the most complicated T dependence of $\varepsilon(T)$, showing two additional features at $\sim$19 and $\sim$8 K as evident in $\varepsilon(T)$ at zero H in Fig. 3(b). Furthermore, $\mathrm{DyMn_2O_5}$ is the most magnetically isotropic [see Fig. 1(b)]. These characteristics as well as the enhanced MD effect consistently indicate that the $\mathrm{DyMn_2O_5}$ system is most magnetically/structurally "soft" [26].

In summary, we have discovered a CMD effect in multiferroics $R\mathrm{Mn_2O_5}$ where the magnetic transitions are closely coupled with dielectric transitions. It appears that the CMD effects are intimately associated with the unique commensurate-incommensurate magnetic transition in the system. This correlation between the high sensitivity of the dielectric constant to H and the incommensurability of magnetic/lattice modulations provide a new, important means to tune dielectric properties with external parameters.

This work was supported by NSF-DMR-0103858.

[1] G. A. Smolenskii and I. E. Chupis, Usp. Fiz. Nauk **137**, 415 (1982) [Sov. Phys. Usp. **25**, 475 (1982)].
[2] H. Schmid, Ferroelectrics **162**, 317 (1994).
[3] R. E. Cohen, J. Phys. Chem. Solids **61**, 139 (2000).
[4] V. J. Folen, G. T. Rado, and E. W. Stalder, Phys. Rev. Lett. **6**, 607 (1961).
[5] J. Kishigami, N. Mori, and E. Sawaguchi, J. Magn. Magn. Mater. **31–34**, 785 (1983).
[6] Z. J. Huang, Y. Cao, Y. Y. Sun, Y. Y. Xue, and C. W. Chu, Phys. Rev. B **56**, 2623 (1997).
[7] M. N. Baibich, J. M. Broto, A. Fert, F. Nguyen Van Dau, F. Petroff, P. Eitenne, G. Creuzet, A. Friederich, and J. Chazelas, Phys. Rev. Lett. **61**, 2472 (1988).
[8] E. E. Fullerton, M. J. Conover, J. E. Mattson, C. H. Sowers, and S. D. Bader, Phys. Rev. B **48**, 15 755 (1993).
[9] E. Dagotto, *Nanoscale Phase Separation and Colossal Magnetoresistance*, Springer Series in Solid-State Sciences (Springer, Berlin, 2002), p. 136.
[10] K. T. McCarthy, A. F. Hebard, and S. B. Arnason, Phys. Rev. Lett. **90**, 117201 (2003).
[11] T. Kimura, S. Kawamoto, I. Ymada, M. Azuma, M. Takano, and Y. Tokura, Phys. Rev. B **67**, 180401 (2003).
[12] G. Lawes, A. P. Ramirez, C. M. Varma, and M. A. Subramanian, Phys. Rev. Lett. **91**, 257208 (2003).
[13] T. Kimura, T. Goto, H. Shintani, K. Ishizaka, T. Arima, and Y. Tokura, Nature (London) **426**, 55 (2003).
[14] I. Kagomiya, H. Kimura, Y. Noda, and K. Kohn, J. Phys. Soc. Jpn. **70**, Suppl. A, 145 (2001).
[15] B. M. Wanklyn, J. Mater. Sci. **7**, 813 (1972).
[16] E. I. Golovenchits, N. V. Morozov, V. A. Sanina, and L. M. Sapozhnikova, Fiz. Tverd. Tela (Leningrad) **34**, 108 (1992) [Sov. Phys. Solid State **34**, 56 (1992)].
[17] K. Saito and K. Kohn, J. Phys. Condens. Matter **7**, 2855 (1995).
[18] I. Nowik, H. J. Williams, L. G. Van Uitert, and H. J. Levinstein, J. Appl. Phys. **37**, 970 (1966).
[19] M. Schieber, A. Grill, I. Nowik, B. M. Y. Wanklyn, R. C. Sherwood, and L. G. Van Uitert, J. Appl. Phys. **44**, 1864 (1973).
[20] Y. Koyata and K. Kohn, Ferroelectrics **204**, 115 (1997).
[21] L. N. Baturov, B. I. Al'shin, and Yu. N. Yarmukhamedov, Fiz. Tverd. Tela (Leningrad) **20**, 2254 (1978) [Sov. Phys. Solid State **20**, 1300 (1978)].
[22] A. Inomata and K. Kohn, J. Phys. Condens. Matter **8**, 2673 (1996).
[23] A. Sawada, S. Ohya, Y. Ishibashi, and Y. Takagi, J. Phys. Soc. Jpn. **38**, 1408 (1975).
[24] A. Sawada and M. Tomatsu, Ferroelectrics **137**, 297 (1992).
[25] C. Wilkinson, F. Sinclair, P. Gardner, J. B. Forsyth, and B. M. R. Wanklyn, J. Phys. C **14**, 1671 (1981).
[26] W. L. McMillan, Phys. Rev. B **12**, 1187 (1975).
[27] P. B. Littlewood and T. M. Rice, Phys. Rev. Lett. **48**, 27 (1982).
[28] Yu. F. Popov, A. M. Kadomtseva, G. P. Vorob'ev, V. A. Sanina, M.-M. Tehranchi, A. K. Zvezdin, A. K. Zvezdin, J. Magn. Magn. Mater. **188**, 237 (1998).